

Theory for photon statistics of random lasers

M. Patra*

Instituut-Lorentz, Universiteit Leiden, Postbus 9506, 2300 RA Leiden, The Netherlands

(Received 15 May 2001; revised manuscript received 9 November 2001; published 21 March 2002)

A theory for the photon statistics of a random laser is presented. Noise is described by Langevin terms, where fluctuations of both the electromagnetic field and of the medium are included. The theory is valid for all lasers with small outcoupling when the laser cavity is large compared to the wavelength of the radiation. The theory is applied to a chaotic laser cavity with a small opening. It is known that a large number of modes can be above threshold simultaneously in such a cavity. It is shown that the amount of fluctuations is increased above the Poissonian value by an amount that depends on the number of modes above threshold.

DOI: 10.1103/PhysRevA.65.043809

PACS number(s): 42.50.Lc, 42.65.Sf, 42.60.Da

I. INTRODUCTION

A random laser is a laser where the necessary feedback is not due to mirrors at the ends of the laser but due to random scattering inside the medium [1–3]. It was long argued about how to distinguish such a random laser from a random medium with amplified spontaneous emission (ASE)—in the former, the randomness is essential for providing feedback, whereas in the latter, scattering only increases the dwell time in the medium and thus the amplification factor. Two years ago, the first experimental proof of a random laser was given [4]. It was demonstrated that the lasing action was indeed due to the randomness of the medium, by measuring the emitted radiation at different points on the surface of the sample and showing that the peaks in the radiation spectrum were completely different at different points.

Earlier experiments [5–7] were only able to prove ASE in random media, frequently referred to as “laserlike emission.” In a medium with saturation both laser action and ASE lead to a dramatic narrowing of the emitted light profile upon crossing some threshold so that this criterion does not necessarily signal a laser. Most “traditional lasers” are characterized by emitting coherent radiation above threshold so that considering only the intensities and forgetting about the fluctuation properties is insufficient. Recently the first two measurements on the photon statistics of a random laser have been published. Papazoglou and co-workers report that the emitted radiation becomes only partially coherent [8] whereas Cao *et al.* report that the statistics become completely Poissonian [9].

The theoretical description of random lasers has in the past focused on the light intensity inside in the laser. Photons were considered as classical particles that diffuse or move in some other way repeatedly through the sample while being amplified. (The literature on this and similar methods is vast, some more general, some focusing more towards a particular system; see, e.g., Ref. [10] for one of the earlier papers.) In this way the intensity of the emitted radiation can be computed, confirming the observed narrowing of the emission

line far above threshold. No results for the fluctuation properties, however, can be derived in this way. Recently, random lasers are also simulated by the finite-difference time-domain method [11]. While this method, in principle, can incorporate quantum fluctuations on a microscopic level, the computational effort is prohibitively large, so that at most two-dimensional samples can be treated (see, e.g., Ref. [12]), and most of its value is for one-dimensional applications (see, e.g., Ref. [13]). Furthermore, only short time series can be computed with acceptable effort so that the fluctuation properties of the emitted radiation are not accessible. A different analytical approach to noise in random lasers has recently been put forward by Hackenbroich *et al.* [14]. Since they do not include mode competition, their work is only applicable near threshold.

For a linear medium, i.e., a medium where, in contrast to a laser, saturation effects can be neglected, the statistics of the emitted radiation can be computed directly, e.g., by the method of input-output relations [15]. No theory of comparable power exists for lasers. The theoretical treatment of “nontrivial” lasers has in the past focused on the Petermann factor (see Refs. [16–18] for a definition). It is a geometry-related factor that describes by how much the excess noise of the emitted radiation is larger than that for a “simple” single-mode laser—*assuming* that the nontrivial laser behaves the same way as a single-mode laser, which is basically equivalent to neglecting mode-competition effects. (It should be stressed that the Petermann factor only gives information about the radiation far above threshold; it gives no information on threshold behavior.) Since the Petermann factor is a geometrical factor it can be computed for a linear medium and then used for the corresponding system filled with a medium with saturation. The Petermann factor has been derived for arbitrary geometries (see, e.g., Refs. [19,20]), but also random media could be treated [21–23].

There thus is a need for a theory that allows one to compute the photon statistics of the emitted light for “nontrivial” lasers, in particular, this includes random lasers. In this paper such a theory based on Langevin terms, also referred to as Langevin noise sources, is presented. Langevin terms have successfully been used to describe the radiation properties of linear media from a microscopic model [20]. On a higher level, they were used to describe random linear amplifying media [24] where the Langevin terms included both fluctua-

*Present address: Laboratory for Computational Engineering, Helsinki University of Technology, P.O. Box 9400, 02015 HUT, Finland.

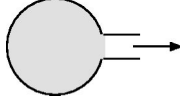


FIG. 1. A (chaotic) cavity is coupled to the outside via a small opening. The cavity is filled with an amplifying medium. The light emitted through the opening is detected.

tions of the electromagnetic field and sample-to-sample fluctuations of the properties of the random medium. None of these theories included saturation effects of the medium so that they break down when the lasing threshold is approached. Apart from saturation effects for a single mode, a large number of modes can be above threshold simultaneously [25], so that mode competition is important and cannot be neglected.

This paper is organized as follows. In Sec. II the model for the photon statistics inside the laser is described and the model equations are derived. These are then solved in Secs. III and IV. Section V adds the necessary modifications to go from the fluctuations inside the laser to the fluctuations of the photocurrent emitted by the laser. Until this point all results are valid for arbitrary lasers, provided that the outcoupling is weak and the volume of the lasing medium is much larger than the cube of the wavelength. In Sec. VI we show how to apply the formalism developed in this paper to three exemplary systems and demonstrate thereby that it can indeed describe all relevant properties of lasing action. In Sec. VII the random laser is treated and its photon statistics are computed. In Sec. VIII we try to explain the experimental results mentioned above. We conclude in Sec. IX.

II. MODEL

We consider a optical cavity that is coupled to the outside by an opening that is small compared to the wavelength of the emitted radiation (see Fig. 1). Since the opening is small, there exist well-defined modes in the cavity, each with a well-defined eigenfrequency ω_i , $i = 1, \dots, N_p$, and an eigenmode profile $\Theta_i(\vec{r})$, and all modes are nonoverlapping [33] (In the language of random lasers, this is a “resonant-feedback laser.”) Each mode i thus can be described by the number n_i of photons in it. Photons in mode i can escape through the opening with rate g_i .

The cavity is filled with an amplifying medium. The medium is modeled by a four-level laser dye (see Fig. 2), where

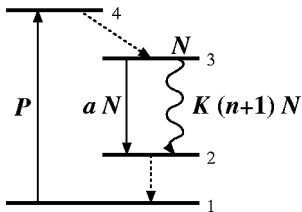


FIG. 2. Amplification is modeled by a four-level system, where lasing action (marked by the wiggly line) is from the third to the second level. Dashed lines mark transitions that are much faster than the other ones and thus need not be included in the description.

the lasing transition is from the third to the second level. The transition from the second level to the ground level is assumed to be so fast that the second level is always empty. The density of excited atoms (i.e., atoms in the third level) at point \vec{r} in the cavity is $N(\vec{r})$. Excitations are created by pumping with rate $P(\vec{r})$ and can be lost nonradiatively with rate $a(\vec{r})$.

Coupling between the electromagnetic field and the medium depends on two quantities, namely, the eigenmode profile $\Theta_i(\vec{r})$ of mode i , and the transition matrix element $w(\omega)$ of the atomic transition $3 \rightarrow 2$. [Frequently $w(\omega)$ will be a Lorentzian centered around some frequency Ω .] The coupling of mode i to the medium at point \vec{r} is then given by $K_i(\vec{r}) \equiv w(\omega_i) |\Theta_i(\vec{r})|^2$.

The semiclassical equations of motion for n_i and $N(\vec{r})$ are (the time argument for all quantities has been suppressed)

$$\dot{n}_i = -g_i n_i + \int d^3r (n_i + 1) K_i(\vec{r}) N(\vec{r}), \quad (1a)$$

$$\dot{N}(\vec{r}) = P(\vec{r}) - a(\vec{r}) N(\vec{r}) - \sum_{i=1}^{N_p} (n_i + 1) K_i(\vec{r}) N(\vec{r}). \quad (1b)$$

“Semiclassical” means that all emission events, pumping events, etc. are assumed to be deterministic, with spontaneous emission described by the addition of a virtual photon to n_i when computing the transition rates [34].

To include the randomness of all processes, Langevin terms have to be added to Eq. (1). The four random processes are the escape of photons (described by the Langevin term Γ_i), pumping [described by $\Phi(\vec{r})$], relaxation of the medium [described by $\alpha(\vec{r})$], and emission of a photon into mode i at point \vec{r} [described by $\Psi_i(\vec{r})$]. Each of these terms has zero mean and a correlator that follows from the assumption that the elementary stochastic processes have independent Poisson distributions, hence

$$\langle \Gamma_i(t) \Gamma_j(t') \rangle = \delta_{ij} \delta(t - t') g_i \langle n_i \rangle, \quad (2a)$$

$$\langle \alpha(\vec{r}, t) \alpha(\vec{r}', t') \rangle = \delta^3(\vec{r} - \vec{r}') \delta(t - t') a(\vec{r}) \langle N(\vec{r}) \rangle, \quad (2b)$$

$$\langle \Phi(\vec{r}, t) \Phi(\vec{r}', t') \rangle = \delta^3(\vec{r} - \vec{r}') \delta(t - t') \langle P(\vec{r}) \rangle, \quad (2c)$$

$$\langle \Psi_i(\vec{r}, t) \Psi_j(\vec{r}', t') \rangle = \delta_{ij} \delta^3(\vec{r} - \vec{r}') \delta(t - t') K_i(\vec{r}) \times \langle (n_i + 1) N(\vec{r}) \rangle. \quad (2d)$$

Equation (2d) corresponds with the correlator given in Eq. (5b) of Ref. [24].

Adding the terms from Eq. (2) to Eq. (1) gives the complete equations of motion,

$$\dot{n}_i = -g_i n_i + \Gamma_i + \int d^3r (n_i + 1) K_i(\vec{r}) N(\vec{r}) + \int d^3r \Psi_i(\vec{r}), \quad (3a)$$

$$\begin{aligned} \dot{N}(\vec{r}) = & P(\vec{r}) + \Phi(\vec{r}) - a(\vec{r})N(\vec{r}) + \alpha(\vec{r}) \\ & - \sum_{i=1}^{N_p} (n_i + 1)K_i(\vec{r})N(\vec{r}) - \sum_{i=1}^{N_p} \Psi_i(\vec{r}). \end{aligned} \quad (3b)$$

The sign of the Langevin terms may be chosen freely as long as the term $\Psi_i(\vec{r})$ has the opposite sign in the equations for \dot{n} and \dot{N} .

III. LINEARIZATION

Equation (3) cannot be solved by direct numerical methods since Langevin terms cannot be represented as “real” numbers. The only practicable way to proceed is to linearize the equations. First, we write $n_i = \bar{n}_i + \delta n_i$ and $N(\vec{r}) = \bar{N}(\vec{r}) + \delta N(\vec{r})$, where $\bar{n}_i \equiv \langle n_i \rangle$ and $\bar{N}(\vec{r}) = \langle N(\vec{r}) \rangle$ are the average solutions. We assume that these average solutions are identical to the solutions of the deterministic rate equation (1). This is equivalent to the factorizing approximation $\langle n_i N(\vec{r}) \rangle \approx \langle n_i \rangle \langle N(\vec{r}) \rangle$. For a single-mode cavity like that used in cavity QED this is a bad approximation, leading to errors of up to a factor 1/4 in the computed average photon density, but if the number of modes in the cavity is large—which is the case that we are interested in—this factorization is valid [28].

Inserting this solution, Eq. (3) can be reformulated so that only δn_i and $\delta N(\vec{r})$ remain as variables. Linearization means that only terms proportional to δn_i or $\delta N(\vec{r})$ are kept, i.e., terms proportional to $\delta n_i \delta N(\vec{r})$ are omitted. (This is justified as long as the variance is sufficiently smaller than the mean. This condition is equivalent to the validity of the factorizing approximation used above. It can be checked self-consistently from the computed results.) This way one arrives at an equation for the fluctuations alone, where the coefficients depend on the average solution,

$$\begin{aligned} \delta \dot{n}_i = & -g_i \delta n_i + \Gamma_i + \int d^3 \vec{r} (\bar{n}_i + 1) K_i(\vec{r}) \delta N(\vec{r}) \\ & + \int d^3 \vec{r} \delta n_i K_i(\vec{r}) \bar{N}(\vec{r}) + \int d^3 \vec{r} \Psi_i(\vec{r}), \end{aligned} \quad (4a)$$

$$\begin{aligned} \delta \dot{N}(\vec{r}) = & \Phi(\vec{r}) - a(\vec{r}) \delta N(\vec{r}) + \alpha(\vec{r}) - \sum_i (\bar{n}_i + 1) K_i(\vec{r}) \delta N(\vec{r}) \\ & - \sum_i \delta n_i K_i(\vec{r}) \bar{N}(\vec{r}) - \sum_{i=1}^{N_p} \Psi_i(\vec{r}). \end{aligned} \quad (4b)$$

For convenience, we will label the sum of the Langevin terms in Eq. (4a) as f_i and the sum in Eq. (4b) as $g(\vec{r})$. Evaluating the Langevin terms from Eq. (2) at the average solutions \bar{n} and \bar{N} gives

$$\langle f_i f_j \rangle = \delta_{ij} \left[g_i \bar{n}_i + \int d^3 \vec{r} (\bar{n}_i + 1) K_i(\vec{r}) N(\vec{r}) \right] = 2 \delta_{ij} g_i \bar{n}_i, \quad (5a)$$

$$\begin{aligned} \langle g(\vec{r}) g(\vec{r}') \rangle = & \delta^3(\vec{r} - \vec{r}') \left[a(\vec{r}) P(\vec{r}) + \bar{N}(\vec{r}) \right. \\ & \left. + \sum_{i=1}^{N_p} (\bar{n}_i + 1) K_i(\vec{r}) \bar{N}(\vec{r}) \right] \\ = & 2 \delta^3(\vec{r} - \vec{r}') P(\vec{r}), \end{aligned} \quad (5b)$$

$$\langle f_i g(\vec{r}) \rangle = -(\bar{n}_i + 1) K_i(\vec{r}) \bar{N}(\vec{r}). \quad (5c)$$

IV. DISCRETIZATION AND NUMERICAL SOLUTION

We now discretize the equations in space by picking points \vec{r}_j , $j = 1, \dots, N_s$. Defining $K_{ij} \equiv K_i(\vec{r}_j)$ and $N_j \equiv N(\vec{r}_j)$ (analogously for all other quantities), the stationary densities \bar{n}_i and \bar{N}_j from Eq. (1) are the solution of the equations

$$g_i \bar{n}_i = \sum_{j=1}^{N_s} (\bar{n}_i + 1) K_{ij} \bar{N}_j \quad (i = 1, \dots, N_p), \quad (6a)$$

$$P_j = a_j \bar{N}_j + \sum_{i=1}^{N_p} (\bar{n}_i + 1) K_{ij} \bar{N}_j \quad (j = 1, \dots, N_s). \quad (6b)$$

This equation cannot be solved analytically but a numerical solution is straightforward (even though it may be numerically expensive if N_p and/or N_s are large).

Equation (4) now becomes a linear ordinary differential equation,

$$\begin{aligned} \frac{d}{dt} \begin{pmatrix} \delta n_i \\ \delta N_j \end{pmatrix} = & \begin{pmatrix} -g_i + \sum_j K_{ij} \bar{N}_j & (\bar{n}_i + 1) K_{ij} \\ -K_{ij} \bar{N}_j & -a_j - \sum_i (\bar{n}_i + 1) K_{ij} \end{pmatrix} \\ & \times \begin{pmatrix} \delta n_i \\ \delta N_j \end{pmatrix} + \begin{pmatrix} f_i \\ g_j \end{pmatrix}, \end{aligned} \quad (7)$$

where it is understood that all indices i run from 1 to N_p and all indices j from 1 to N_s , so that the previous equation can be written as an $(N_p + N_s)$ -dimensional matrix equation $\delta \dot{\mathcal{N}} = \mathcal{A} \delta \mathcal{N} + \mathcal{L}$. Computing from \mathcal{A} its matrix \mathcal{U} of eigenvectors and its vector \mathcal{E} of eigenvalues, the formal solution can immediately be written down as

$$\delta \mathcal{N}_j(t) = \sum_{k, l=1}^{N_p + N_s} \int_{-\infty}^t dt' \mathcal{U}_{jk} e^{\mathcal{E}_k(t-t')} \mathcal{U}_{kl}^{-1} \mathcal{L}_l(t'). \quad (8)$$

Since the vector \mathcal{L} consists of Langevin terms, a numerically computed solution of Eq. (8) is not meaningful. Instead of $\delta \mathcal{N}_j(t)$ alone one has to consider correlators $\langle \delta \mathcal{N}_j(t) \delta \mathcal{N}_{j'}(t) \rangle$. Noting that the \mathcal{L} 's are delta correlated in time and that we are interested in $t \rightarrow \infty$ (as we are not interested in intermittent behavior when switching on the laser), we arrive at

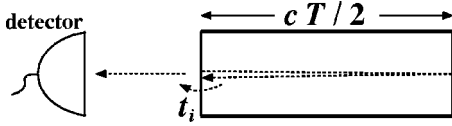


FIG. 3. The loss rate of photons inside the cavity is given by the ratio of the probability t_i that a photon incident on the outcoupling mirror is transmitted and the time T needed for one round-trip through the cavity. The photons emitted from the cavity are detected by an ideal photodetector.

$$\langle \delta \mathcal{N}_j \delta \mathcal{N}_{j'} \rangle = - \sum_{k,l,m,n=1}^{N_p+N_s} \frac{\mathcal{U}_{jm} \mathcal{U}_{j'n} \mathcal{U}_{mk}^{-1} \mathcal{U}_{nl}^{-1}}{\mathcal{E}_m + \mathcal{E}_n} \langle \mathcal{L}_k \mathcal{L}_l \rangle. \quad (9)$$

Inserting the expectation values of the correlators from Eq. (5) gives the final result where a numerical solution is easy once the average solution \bar{n}_i , \bar{N}_j is known. ($\langle \mathcal{L}_k \mathcal{L}_l \rangle$ has to be evaluated at the average solution and thus does not depend on time.)

V. OUTCOUPLING

So far we have considered the number of photons n_i in the i th mode *inside* the cavity. For practical purposes one is more interested in the photocurrent I emitted *from* the cavity. (I gives the number of photons emitted per unit time and is thus equal to the photon flux integrated over the entire cross-sectional area.) Even though the photons from different modes i are emitted through the same opening, each mode has a distinct frequency ω_i so that the modes are easily distinguished on the outside. We can thus define the photocurrent $j_i(t) \equiv \bar{j}_i + \delta j_i(t)$ through the opening due to the i th mode in the cavity. The photocurrent can, for example, be measured by an (ideal) photodetector that absorbs the emitted photons. The fluctuations of the photocurrent within some time τ (we assume the limit $\tau \rightarrow \infty$) are quantified by the noise power

$$P_i = \lim_{\tau \rightarrow \infty} \frac{1}{\tau} \int_{-\tau/2}^{\tau/2} dt \delta j_i(0) \delta j_i(t). \quad (10)$$

The ratio $\mathcal{F}_i = P_i / \bar{j}_i$ is called the Fano factor and is frequently used to describe the fluctuation properties of optical radiation.

In Sec. II we have introduced the loss rates g_i . From their definition it is obvious that the mean photocurrent \bar{j}_i is

$$\bar{j}_i = g_i \bar{n}_i. \quad (11)$$

To also compute the fluctuations δj_i we need to treat the outcoupling in more detail. In a traditional laser (see Fig. 3) the loss rate g_i is given by the ratio of the transmission probability t_i (in classical optics referred to as “transmittivity”) through the outcoupling mirror and the round-trip time T through the cavity,

$$g_i = t_i / T. \quad (12)$$

The transmission through the outcoupling mirror changes the noise of the signal compared to the noise inside the cavity, and the Fano factor of the emitted radiation is [26]

$$\mathcal{F}_i = t_i \frac{\langle \delta n_i \delta n_i \rangle}{\bar{n}_i} + 1 - t_i. \quad (13)$$

This equation can, apart from following the quantum-optical approach of Ref. [26], also be understood by the following simple argument: The fraction $\langle \delta n_i \delta n_i \rangle / \bar{n}_i$ on the right-hand side is the Fano factor of the radiation trapped inside the cavity in mode i . With probability t_i the detector will “see” the radiation inside the cavity, and with probability $1 - t_i$ it will see reflected vacuum fluctuations (which have a Fano factor equal to 1).

The Fano factor for a measurement where the photons emitted from the cavity in all modes are detected simultaneously is

$$\mathcal{F} = \frac{\sum_i t_i^2 \langle \delta n_i \delta n_i \rangle}{\sum_i t_i \bar{n}_i} + \frac{\sum_i t_i (1 - t_i) \bar{n}_i}{\sum_i t_i \bar{n}_i}. \quad (14)$$

It is immediately obvious that t_i and g_i can for a traditional laser be identified by properly choosing the unit of time (for the simple laser from Fig. 3: by choosing T as the unit of time). We will show in Sec. VII that this is also possible for a random laser. In the following, when giving numerical values or distribution functions for g_i this identification has been made.

VI. COMPARISON OF LASING REGIMES

To demonstrate the application of the formalism presented in this paper and the validity of the approximations made in this paper we first want to discuss three simple cases not involving random media. For simplicity we set $a \equiv w \equiv 1$, $N_s = N_p$, and $K \equiv \text{const}$. This reduces the number of parameters significantly without reducing the physical content.

The physical features of a laser (in contrast to a linear amplifier) are easily understood in the following picture: A certain number of excited atoms are created by pumping within a certain time, and each of those excitations has to be “consumed” either by nonradiative relaxation or by emitting one photon from the cavity. For high photon number in the cavity, nonradiative relaxation can be neglected, and each pumping event eventually leads to the emission of one photon from the cavity. The fluctuations of the *integrated* photocurrent are thus equal to the fluctuations of the pump source, assumed to be Poissonian throughout this paper.

In Fig. 4(a) the single-mode laser ($N_p = 1$) with a small opening ($g = 10^{-2}$) is treated. The computed curve reproduces the features of a “traditional” laser. The precise location of the maximum is somewhat off (see the discussion of the factorization approximation above, or refer to Ref. [27] for a more detailed discussion of the effects of different approximations on the computed curve near the lasing thresh-

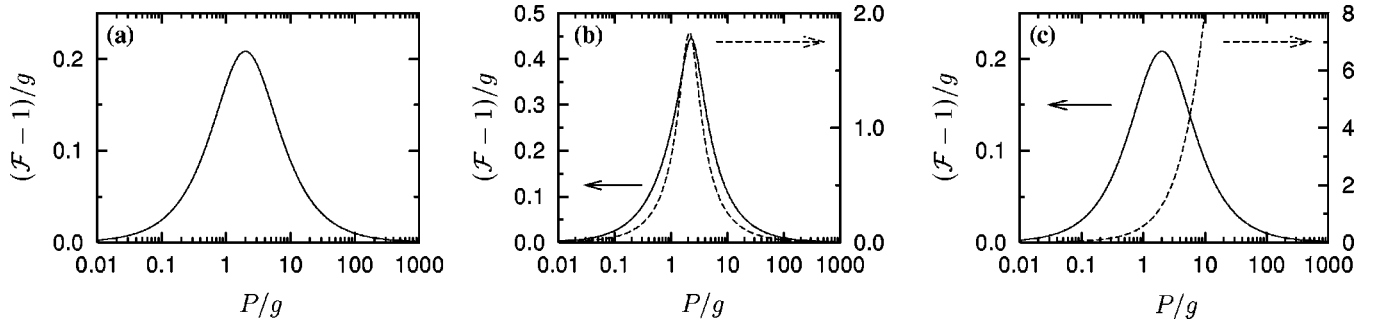


FIG. 4. Comparison of the Fano factor \mathcal{F} for three different conditions. The left axis (solid line) depicts the Fano factor for the integrated emitted radiation, the right axis (dashed line) for the lasing mode only. (a) Laser with just a single mode. (b) Laser with a cavity supporting ten modes where one mode is coupled out much less than the others, thus effectively modeling a single-mode laser with $\beta \approx 0.1$. (c) Laser with ten identical modes.

old), but its height reproduces the exact quantum-mechanical value well. For high values of the pumping, the photon statistics of the emitted radiation becomes Poissonian, as qualitatively explained above.

In Fig. 4(b) we have modeled a laser with one mode coupled to the outside with $g=10^{-2}$ and the other nine modes with $g=10^{-1}$, hence $N_p=10$. (The value $g=10^{-2}$ was chosen for scaling the axes of the figure.) The mode with the smallest g will be the lasing mode, whereas radiation in the other modes quickly escapes to the outside so that no significant number of photons can accumulate in those modes. This basically models a single-mode laser where only a fraction $\beta=1/N_p$ of the spontaneous radiation is emitted into the lasing mode. (β is called the spontaneous-emission factor. An ideal cavity-QED laser has $\beta=1$ whereas a semiconductor laser can have a β as low as $\beta=10^{-8}$.) The behavior is similar to Fig. 4(a), except that the peak of the Fano factor of the lasing mode is larger by about a factor of 8. For small β , one expects a scaling $\propto \beta^{-1/2} \approx 3$ [28] but $\beta=1$ and $\beta=0.1$ are too large for that scaling to be exactly valid.

In Fig. 4(c) the system is kept at $N_p=10$ with all $g_i \equiv 10^{-2}$. The total radiation depicts the same qualitative behavior as for the two cases presented so far but the radiation emitted by the lasing mode alone (in this case, by an arbitrary but fixed mode) depicts a completely different picture: The Fano factor diverges as the pumping is increased. This is easily understood by the qualitative description given above. For high pumping, every pump excitation eventually results in one photon being emitted from the cavity, but if there are several lasing modes the photon still has the freedom to choose one of those modes. These additional fluctuations can be so large that they eventually lead to a very large Fano factor for large pumping. (It is obvious that the Langevin approach will break down eventually if the fluctuations become too large, as explained above.)

The three test cases show that the model presented here is able to explain all relevant features of a laser.

VII. RANDOM LASER

A random laser is a laser where the feedback is not due to mirrors at the ends of the laser but due to chaotic scattering, either caused by scatterers placed at random positions or by a

chaotic shape of the cavity [1,3]. If the mean outcoupling is weak, a large number of modes in the cavity can be above threshold simultaneously [25]. As seen above, mode competition introduces additional noise into the modes. However, even if there are several modes above threshold, there only will be mode competition if the modes are spatially overlapping and thus are “eating” from the same excitations. The main purpose of this paper is to answer the question of whether in a random laser there is a relevant level of mode-competition noise or whether the radiation emitted in a laser line approaches Poissonian statistics for strong pumping—both statements are mutually exclusively.

We consider a chaotic cavity as depicted in Fig. 1 with a small opening to the outside. This problem becomes a stochastic problem by considering an ensemble of cavities with small variations in shape or scatterer positions. The coefficients appearing in Eq. (6) thus become random quantities. The statistics of these coefficients for a chaotic cavity with a small opening is known [29,30]. The mean loss rate \bar{g} of a cavity with volume V through a hole of diameter d at frequency ω is [31]

$$\bar{g} = \frac{16\pi^2 d^6 \omega^6}{c^6} \frac{\pi^2 c^3}{\omega^2 V^2} \equiv \bar{t} \delta. \quad (15)$$

δ is the level spacing of the cavity. Its inverse $1/\delta$ is the time needed to explore the entire phase space inside the cavity and can be identified with the round-trip time introduced for a “traditional laser” in Eq. (12).

In a chaotic cavity the modes $\Theta_i(\vec{r})$ can be modeled as random superpositions of plane waves [32]. This implies a Gaussian distribution for $\Theta_i(\vec{r})$ at any point \vec{r} [35]. The loss rate g_i is proportional to the square of the gradient of $\Theta(\vec{r})$ normal to the opening at the opening, hence its distribution is

$$\mathcal{F}(g_i) = \frac{e^{-2g_i/\bar{g}}}{\sqrt{2\pi g_i \bar{g}}} \quad (16)$$

and g_i and g_j are uncorrelated for $i \neq j$.

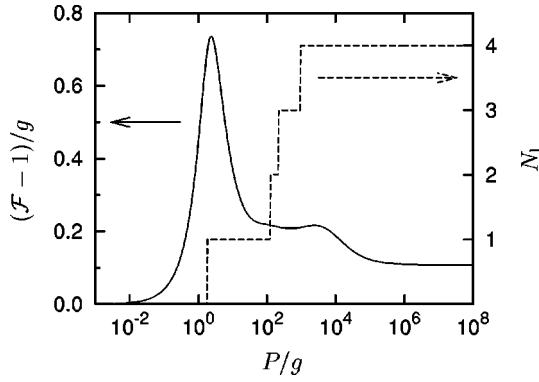


FIG. 5. Fano factor of the radiation emitted from the (primary) lasing mode (left axis, solid line) of some particular sample. The right axis (dashed line) depicts the number of modes above lasing threshold. Each additional mode crossing the threshold increases the Fano factor of the primary lasing mode.

It should be noted that the level spacing δ is no random quantity, so that g_i and t_i can be identified by choosing $1/\delta$ as the unit of time.

For simplicity we assume that the amplification profile $w \equiv 1$ so that the distribution of the eigenfrequencies is not needed to compute K_{ij} . (The distribution is known [29] so that an extension to nonconstant w is straightforward.)

Figure 5 shows the computed Fano factor for a particular sample from this ensemble ($N_p = 10$, $\bar{g} = 0.5$, but it should be kept in mind that the value of g of the lasing mode is much smaller than \bar{g} [21,23]). This kind of curve is typical for all members of the ensemble, while the precise shape varies. When the first mode crosses the lasing threshold, the Fano factor goes through a maximum. While there is a global decrease with increasing pumping, additional peaks are superimposed each time another mode crosses the lasing threshold. (In the following a mode is considered to be above lasing threshold if it contains at least two photons, but the results are basically independent of whether one chooses one, two, or ten photons.) The Fano factor approaches the value 1 along with some finite difference. Mode-competition noise thus gives a contribution to the noise but there still exists a lasing threshold that is well defined by a peak of \mathcal{F} .

Similarly to computing the fluctuations of the Fano factor, it is possible to compute the fluctuations $\delta N(\vec{r})$ of the density of excited atoms directly from Eq. (9). Figure 6 depicts the computed fluctuations for the entire cavity (dashed lines) as well as for the point \vec{r}_1 where the eigenmode profile $\Theta_l(\vec{r})$ of the primary lasing mode has the largest magnitude. The former quantity peaks at a significantly larger pumping P , which is immediately understood by noticing that the primary lasing mode affects only part of the total cavity, and a significant part of the cavity is left “untouched” until more modes have crossed the lasing threshold.

The two global quantities depicted, $\langle [\int d^3\vec{r} \delta N(\vec{r})]^2 \rangle / \int d^3\vec{r} \bar{N}(\vec{r})$ and $\langle \int d^3\vec{r} \delta N^2(\vec{r}) \rangle / \int d^3\vec{r} \bar{N}(\vec{r})$, differ by the inclusion of terms $\langle \delta N(\vec{r}_1) \delta N(\vec{r}_2) \rangle$, $\vec{r}_1 \neq \vec{r}_2$. The different heights of the peaks (the first one is higher) demonstrate that (at least in the relevant interval of P , and on

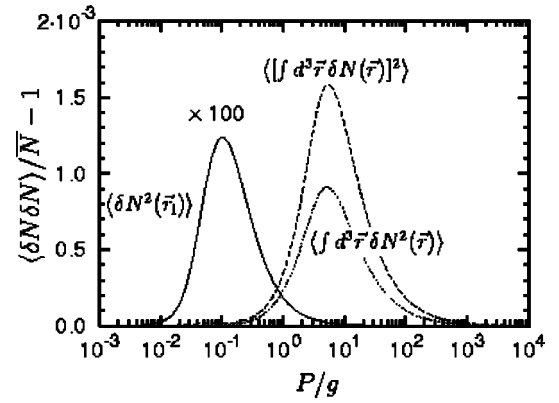


FIG. 6. Fluctuations of the excitation density $N(\vec{r})$ of the medium for the sample from Fig. 5. Depicted are the fluctuations $\langle \delta N^2(\vec{r}_1) \rangle / \bar{N}(\vec{r}_1)$ at the point \vec{r}_1 , where the eigenmode profile of the primary lasing mode has the largest magnitude (solid line, scaled by a factor 100), and the global quantities $\langle [\int d^3\vec{r} \delta N(\vec{r})]^2 \rangle / \int d^3\vec{r} \bar{N}(\vec{r})$ (long dashes) and $\langle \int d^3\vec{r} \delta N^2(\vec{r}) \rangle / \int d^3\vec{r} \bar{N}(\vec{r})$ (short dashes).

average) the density of excited atoms at different positions is positively correlated. This can be understood in the following simple picture: The photon densities n_i and the excitation densities $N(\vec{r})$ are on average negatively correlated since each emission of an extra photon ($\delta n_i > 0$) leads to the de-excitation of an atom [$\delta N(\vec{r}) < 0$] and vice versa, hence $\langle \delta n_i \delta N(\vec{r}) \rangle < 0$. [This has also been confirmed by computing this correlator numerically from Eq. (9)]. Since the excited atoms at different positions communicate only via the radiation field, their density thus has to be positively correlated.

It is difficult to relate the fluctuations of the excitation density of the medium to the properties of the emitted light. With increasing pumping, a peak of $\langle \delta N^2(\vec{r}_1) \rangle / \bar{N}(\vec{r}_1)$ starts to form (cf. Fig. 6) at the same level of pumping as that at which a peak starts to form for the Fano factor \mathcal{F} (cf. Fig. 5), but the location of the maximum of the peak is significantly different for both curves. The complicated interplay between radiation modes and matter in a random laser does not allow for a simple understanding of the relation between these two quantities, and we will not discuss the fluctuations of the medium further in this paper since it focuses on the radiation properties. The complicated structure of the eigenmodes of a chaotic cavity is what makes a random laser fundamentally different from a “traditional” laser.

In the following we will concentrate on the radiation and on the Fano factor far above threshold. P is chosen such that $P/g \approx 10^7$ (remember that the value of g of the lasing mode fluctuates). This is a compromise between a value as large as possible to ensure that the limiting value for $P \rightarrow \infty$ is approached as closely as possible and a not too large value of P to avoid numerical problems (remember that Fig. 5 already spans 11 orders of magnitude).

The main results of a Monte Carlo simulation with $N_p = 10$ are depicted in Fig. 7. The scaled Fano factor does not depend on the size of the opening [Fig. 7(a)], and only weakly depends on the outcoupling constant of the lasing mode [Fig. 7(b)]. As Fig. 7(c) clearly shows, the true depen-

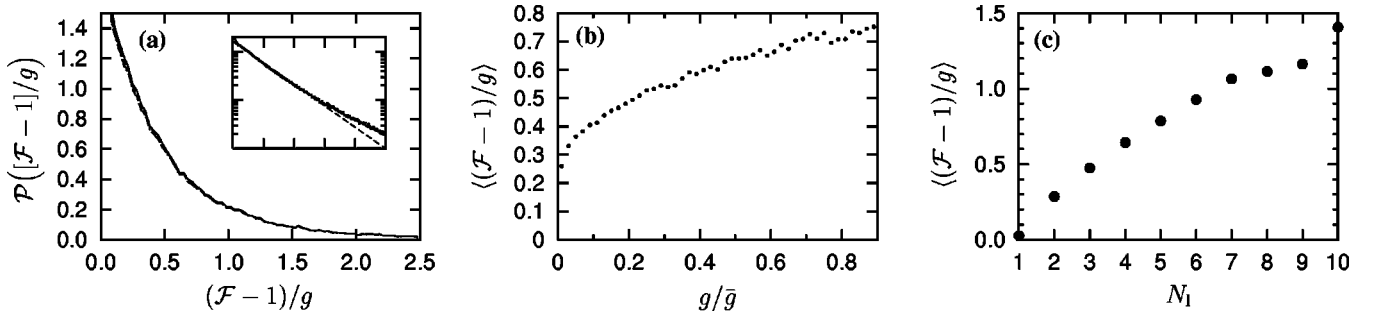


FIG. 7. The value of the Fano factor for the primary lasing mode depends on the number N_1 of cavity modes above laser threshold, not on the other parameters; unless otherwise noted, computed from $\approx 9 \times 10^5$ samples with $\bar{g}=0.1$. (a) Probability distribution of $(\mathcal{F}-1)/g$ for $\bar{g}=0.1, 0.2, \dots, 0.5$. The five curves overlap almost perfectly, thereby demonstrating that the size of the opening does not influence the amount of mode-competition noise generated. (Computed from $\approx 10^5$ samples for each value of \bar{g} with identical realizations for K_{ij} and g_i/\bar{g} for the five runs.) The inset shows the probability distribution from the large set with $\bar{g}=0.1$ plotted logarithmically. (b) Average of the Fano factor as a function of the outcoupling constant g of the lasing mode. (c) Average of the Fano factor as a function of N_1 .

dence is on the number N_1 of modes above threshold. (The weak dependence of the Fano factor on the value of g of the lasing mode can be understood by noting that N_1 is correlated with g of the lasing mode.) The finite value of $\mathcal{F}-1$ thus indeed is due to mode-competition noise, as claimed above.

For larger cavities, i.e., cavities with more modes in it, the distribution of $(\mathcal{F}-1)/g$ changes from a peak near $\mathcal{F}=1$ to one that peaks at a finite value of $(\mathcal{F}-1)/g$, as seen from Fig. 8. As N_p and N_s increase, the effort to numerically compute the average solution from Eq. (6) increases very fast, so that only a comparably small number of realizations were computed ($\approx 20\,000$ for $N_p=50$ and ≈ 4000 for $N_p=150$), explaining the large sampling error in the histograms. [The speed could be increased significantly by developing an optimized algorithm for solving Eq. (6).] For larger N_p the average of $(\mathcal{F}-1)/g$ becomes smaller as the large- \mathcal{F} tail gradually disappears. (From $N_p=10$ to $N_p=150$ the average becomes smaller by about a factor of 2; the average is difficult to compute since it sensitively depends on few samples with large \mathcal{F} .)

VIII. INTERPRETATION OF EXPERIMENTS

Experiments on random lasers are usually explained by the formation of small “virtual” cavities, which can “trap”

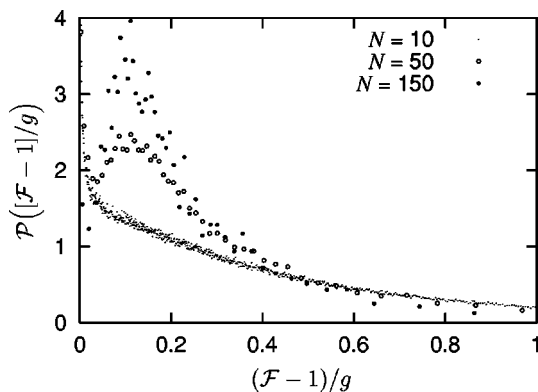


FIG. 8. Distribution of the scaled Fano factor for cavities with different number $N_p=N_s$ of modes.

laser light, so that it is scattered within a small volume many times before it can escape; see Fig. 9. (The linear dimension of such cavities was measured to be of the order of 100 wavelengths [4].) The chaotic cavity used as a model in this paper should be understood as representing one of those virtual cavities. It is not obvious which values of the parameters (N_p , N_s , g_i, \dots) are needed to explain the experiments. In the following we will argue that the important parameters are the average outcoupling \bar{g} and, even more importantly, the probability distribution $\mathcal{P}(g_i/\bar{g})$ as they together determine the number N_1 of modes above lasing threshold.

Above it was shown that N_p and N_s influence the Fano factor only weakly, i.e., only by a factor of 2, and thus by a much smaller factor than the difference observed in the experiments. Even though it was not explicitly discussed in this paper, it is obvious that the choice of $w(\omega)$ and $\Theta_i(\vec{r})$ will not be important either. This leaves \bar{g} and $\mathcal{P}(g_i/\bar{g})$ as parameters to explain the experiments.

In this paper, a random laser is modeled by a chaotic cavity with a small opening. The size of the opening determines the average outcoupling \bar{g} , and all g_i scale linearly with \bar{g} [see Eq. (16)]. For a virtual cavity the average outcoupling cannot be computed in such a simple geometrical way. The outcoupling g_i for the i th mode in such a virtual cavity depends delicately on the positions of the scatterers and the wavelength of that mode. While no theory is available to compute g_i or at least \bar{g} for this case, it is likely that it will be relatively large as individual scatterers cannot be as

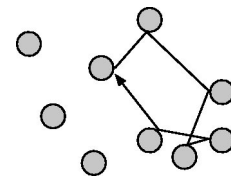


FIG. 9. Small “virtual” cavities can be formed by scatterers in the random medium. Photons can be trapped very efficiently (i.e., small outcoupling) if the distances between the scatterers are compatible with the wavelength of the radiation.

effective as a massive wall with only one small opening.

It was shown in Fig. 7(a) that $\mathcal{F}-1 \propto \bar{g}$. This is valid as long as the size of the opening is small compared to the square of the wavelength. If the opening becomes larger, the modes inside the cavity acquire a finite width (in frequency space) and start to overlap, severely complicating the theory [36], and it is not obvious how the behavior changes. Cao *et al.* [9] speculate that this overlapping prevents the formation of a fixed photon number in one particular mode as photons are constantly exchanged between modes with nearby frequencies. Furthermore, the Petermann factor of the lasing mode becomes significantly large [22], which might or might not increase the amount of fluctuations. While there is no proof that the amount of fluctuations is increased by these two effects, it seems to be obvious that the amount of fluctuations will not decrease due to them. Hence, $\mathcal{F}-1$ will at least increase proportionally to the size of the opening—also for openings that are larger than the region of validity of the theory presented in this paper.

The previous argument assumes that the number N_1 of lasing modes inside a virtual cavity is the same as for a chaotic cavity with a small hole. Mode overlap itself does not change that number, but for a larger opening the distribution function $\mathcal{P}(g_i/\bar{g})$ no longer has the form given by Eq. (16). The form of $\mathcal{P}(g_i/\bar{g})$ sensitively depends on the kind of outcoupling and the number of lasing modes, in turn, sensitively depends on $\mathcal{P}(g_i/\bar{g})$. For example, there already is a large difference between a cavity with one small hole and a cavity with two somewhat smaller holes (so that the total average loss rate is the same in both cases) [25]. It is very well possible that the form of $\mathcal{P}(g_i/\bar{g})$ may look significantly different from Eq. (16) and could depend on many parameters of the sample.

The differences in $\mathcal{P}(g_i/\bar{g})$ and thus in the number of lasing modes are thus the natural candidates to explain the differences observed in the two experiments.

This prediction could, in principle, be checked experimentally by measuring the number of modes above threshold in *one* virtual cavity, but to devise an experimental setup to do this seems very difficult, if at all possible. The sample used by Papazoglou and co-workers [8] should have several spatially overlapping modes above lasing threshold (i.e., some modes above threshold are in the same virtual cavity), whereas in the sample by Cao *et al.* [9] all modes above

lasing threshold should be spatially separated (i.e., be in different virtual cavities). One explanation could be that the sample of Cao *et al.* has more resonant feedback, so that the confinement of the lasing modes is stronger compared to Papazoglou's sample. In the latter, the modes would be extended over a much larger part of the sample (i.e., the virtual cavities are larger), giving them more possibility to overlap.

IX. CONCLUSIONS

In this paper we have developed a theory to compute the fluctuation properties of the radiation of a random laser. While for a standard single-mode laser the emitted radiation becomes coherent far above threshold, the radiation for a random laser fluctuates more. It was shown that this extra noise is due to mode-competition noise, i.e., due to the uncertainty of deciding into which mode a photon is emitted by induced emission. This noise is larger, the higher the number of modes above lasing threshold is.

To be able to create mode-competition noise, the competing modes have to be (at least partially) overlapping. On the other hand, if the profiles of the modes are overlapping too much, usually only one of those modes will be above threshold. The amount of noise created thus is the result of a delicate interplay between these two competing effects. For a random laser modeled by a chaotic cavity filled with a laser dye, this leads to a finite increase of the Fano factor far above threshold, with the precise value depending on the number of modes within the cavity, which are simultaneously above threshold for that particular realization of the disorder. In particular, the emitted radiation becomes coherent if only one mode is above threshold.

Recent experiments on random lasers [8,9] gave conflicting results on whether the noise is increased with respect to the Poissonian value. Even though it is not directly possible to model the differences in the two experiments, the theory presented in this paper suggests that this is due to the differences in the number of modes above threshold. This number depends heavily on the specific system in question, so that the noise properties of a random laser are not universal but depend on the (experimental) setup.

ACKNOWLEDGMENT

Valuable discussions with C.W.J. Beenakker are acknowledged.

-
- [1] D. S. Wiersma, M. P. van Albada, and A. Lagendijk, *Nature (London)* **373**, 203 (1995).
- [2] D. S. Wiersma and A. Lagendijk, *Phys. World* **10**, 33 (1997).
- [3] C. W. J. Beenakker, in *Diffuse Waves in Complex Media*, Vol. 531 of *NATO Advanced Studies Institute, Series C: Mathematical and Physical Sciences*, edited by J.-P. Fouque (Kluwer, Dordrecht, 1999), pp. 137–164.
- [4] H. Cao, Y. G. Zhao, S. T. Ho, E. W. Seelig, Q. H. Wang, and R. P. H. Chang, *Phys. Rev. Lett.* **82**, 2278 (1999).
- [5] W. L. Sha, C.-H. Liu, and R. R. Alfano, *Opt. Lett.* **19**, 1922 (1994).
- [6] N. M. Lawandy, R. M. Balachandran, A. S. L. Gomes, and E. Sauvain, *Nature (London)* **368**, 436 (1994).
- [7] D. Z. Zhang, B. Y. Cheng, J. H. Yang, Y. L. Zhang, W. Hu, and Z. L. Li, *Opt. Commun.* **118**, 462 (1995).
- [8] G. Zacharakis, N. A. Papadogiannis, G. Filippidis, and T. G. Papazoglou, *Opt. Lett.* **25**, 923 (2000).
- [9] H. Cao, Y. Ling, J. Y. Xu, C. Q. Cao, and P. Kumar, *Phys. Rev. Lett.* **86**, 4524 (2001).
- [10] D. S. Wiersma and A. Lagendijk, *Phys. Rev. E* **54**, 4256

- (1996).
- [11] A. Taflove, *Computational Electrodynamics: The Finite-Difference Time Domain Method* (Artech House, Boston, 1995).
- [12] H. Cao, J. Y. Xu, S.-H. Chang, and S. T. Ho, Phys. Rev. E **61**, 1985 (2000).
- [13] X. Jiang and C. M. Soukoulis, Phys. Rev. Lett. **85**, 70 (2000).
- [14] G. Hackenbroich, C. Viviescas, B. Elattari, and F. Haake, Phys. Rev. Lett. **86**, 5262 (2001).
- [15] C. W. J. Beenakker, Phys. Rev. Lett. **81**, 1829 (1998).
- [16] K. Petermann, IEEE J. Quantum Electron. **15**, 566 (1979).
- [17] A. E. Siegman, Phys. Rev. A **39**, 1253 (1989).
- [18] A. E. Siegman, Phys. Rev. A **39**, 1264 (1989).
- [19] P. J. Bardroff and S. Stenholm, Phys. Rev. A **60**, 2529 (1999).
- [20] P. J. Bardroff and S. Stenholm, Phys. Rev. A **61**, 023806 (2000).
- [21] M. Patra, H. Schomerus, and C. W. J. Beenakker, Phys. Rev. A **61**, 023810 (2000).
- [22] K. M. Frahm, H. Schomerus, M. Patra, and C. W. J. Beenakker, Europhys. Lett. **49**, 48 (2000).
- [23] H. Schomerus, K. M. Frahm, M. Patra, and C. W. J. Beenakker, Physica A **278**, 469 (2000).
- [24] E. G. Mishchenko and C. W. J. Beenakker, Phys. Rev. Lett. **83**, 5475 (1999).
- [25] T. S. Misirpashaev and C. W. J. Beenakker, Phys. Rev. A **57**, 2041 (1998).
- [26] M. Patra and C. W. J. Beenakker, Phys. Rev. A **61**, 063805 (2000).
- [27] J. Herzog and J. A. Bergou, Phys. Rev. A **62**, 063814 (2000).
- [28] P. R. Rice and H. J. Carmichael, Phys. Rev. A **50**, 4318 (1994).
- [29] C. W. J. Beenakker, Rev. Mod. Phys. **69**, 731 (1997).
- [30] T. Guhr, A. Müller-Groeling, and H. A. Weidenmüller, Phys. Rep. **299**, 189 (1998).
- [31] H. A. Bethe, Phys. Rev. **66**, 163 (1944).
- [32] M. V. Berry, Phys. Rev. A **10**, 2083 (1977).
- [33] For cavities with symmetries it can happen that two modes have the same eigenfrequency but this is not possible for random cavities due to mode repulsion [29].
- [34] For a cavity with overlapping modes it is unclear whether the “+1” would have to be replaced by “+ K_i ,” where K_i is the Petermann factor of the i th mode. For cavities with a small opening this ambiguity does not arise as for those with $K_i \equiv 1$.
- [35] If space is discretized into N_s points \vec{r}_j , the distribution of $\Theta_i(\vec{r}_j)$ is no longer Gaussian, as $\Theta_i(\vec{r}_j)$ now is the average of $\Theta_i(\vec{r})$ over some region around \vec{r}_j . The most efficient numerical procedure then is to set $\Theta_i(\vec{r}_1), \dots, \Theta_i(\vec{r}_{N_s})$ to a random vector of length 1, i.e., to a column of a random unitary matrix [29].
- [36] Overlapping modes can exchange particles, so a scattering term would need to be included in the equations. Even more problematic is the fact that the eigenmodes of the cavity no longer are orthogonal, the Petermann factor thus is larger than 1 [21–23] and the noise properties change: More noise is emitted into each mode but the noise in different modes is correlated so that the total noise power in the linear regime below threshold stays at the value given by the fluctuation-dissipation theorem. It is not clear how to include this into the framework presented in this paper.